JOURNAL OF Applied Polymer SCIENCE

# Antifouling ultrafiltration membrane fabricated from poly (arylene ether ketone) bearing hydrophilic hydroxyl groups

**Jianhua Zhu,[1,2] Jifu Zheng,[1] Qifeng Zhang,[1] Suobo Zhang[1]**

[1]Key Laboratory of Ecomaterials, Changchun Institute of Applied Chemistry, Chinese Academy of Sciences, Changchun 130022, China

[2]University of Chinese Academy of Sciences, Beijing 100039, China

Correspondence to: S. Zhang (E-mail: sbzhang@ciac.ac.cn) and Q. Zhang (E-mail: qfzhang@ciac.ac.cn)

**ABSTRACT:** A new kind of membrane formation polymer, cardo poly(arylene ether ketone) bearing hydrophilic hydroxyl groups (PEK-OH) was synthesized from the biphenol monomer 2-(2-hydroxyethyl)-3, 3-bis (4-hydroxyphenyl)-isoindolin-1-one (PPH-OH), and 4, 4′-difluorodiphenylketone. PEK-OH asymmetric ultrafiltration membranes were prepared using the immersion coagulation phase inversion method. The PEK-OH membrane prepared using the optimized conditions exhibited a pure water flux of 516 ± 18 $L \cdot m^{-2} \cdot h^{-1}$ and a 99.1 ± 1.4% rejection of bovine serum albumin (BSA) at an operating pressure of 0.1 MPa. The contact angle of PEK-OH membrane was 66.0 ± 2.4 lower than these of the PEK-C membrane (87.0 ± 2.8°, prepared from polymer PEK-C under the same membrane formation condition as PEK-OH membrane) and the UE50 membrane (84.0 ± 1.6°, a commercial PES ultrafiltration membrane). The amount of BSA protein adsorbed to the PEK-OH membrane under static condition was measured to be 3.12 $\mu g \cdot cm^{-2}$, which was greatly lower than that of 88.71 $\mu g \cdot cm^{-2}$ and 74.40 $\mu g \cdot cm^{-2}$ for the PEK-C and the UE50 ultrafiltration membranes, respectively. Under dynamic filtration of BSA experiments, the PEK-OH ultrafiltration membrane showed a 78.3% water flux recovery ratio, while only a 39.7% for the PEK-C membrane and 46.5% for UE50 membrane were detected in the first cycle. After three cycles of BSA and LYZ filtration, the flux recovery ratio of PEK-OH ultrafiltration membrane changed to be stable at 75% and 73%, while that of PEK-C and UE50 ultrafiltration membranes remained declining gradually. Thus, hydrophilic PEK-OH improves antifouling membrane property. © 2015 Wiley Periodicals, Inc. J. Appl. Polym. Sci. **2016**, *133*, 42809.

**KEYWORDS:** hydrophilic polymers; membranes; properties and characterization

Received 31 March 2015; accepted 4 August 2015

**DOI: 10.1002/app.42809**

## INTRODUCTION

Considerable interest in the synthesis of new polymeric materials for the fabrication of membranes applied to separation processes has been generated in recent years.[1–4] In particular, the demand for new materials having high selectivity, high permeability, and chemical resistance has become enormous in the liquid and gas separation fields. Polyetherketone (PEK) represents a class of materials useful for the manufacture of membranes that combine excellent thermal stability in the hot tea separation process and pulp waste water, resistance to acid and base, and good solvent tolerance in organic solvent nanofiltration.[1,2] PEK membranes have been widely used in liquid and gas separation technologies and re-elevated temperature alkaline fuel cells due to good mechanical and film-forming characteristics.[3–5] However, because of its intrinsic hydrophobic character, PEK membranes are easily fouled by many solutes, including proteins, polysaccharides, and humic substances.[6] Fouling deteriorates the performance of membranes due to longer filtration time and shortens membrane life due to the harsh chemical agents required for cleaning.[7,8] In biotechnology and biomedical applications, biofouling may lead to platelet adhesion, aggregation, and coagulation, which restrict the application of PEK in blood-contacting environments. Therefore, it is necessary to modify the PEK membrane to improve its hydrophilicity and biocompatibility.[9]

Modification of PEK membranes with the view of increasing hydrophilicity could be carried out on the membrane surface or in the bulk material.[10,11] Surface modification is considered as a potential route to improve the hydrophilicity or charge properties of the membrane surface. Surface modification methods include coating onto the membrane surface with hydrophilic components [12–14] and grafting polymerization of hydrophilic monomers that chemically attach to the membrane surface.[15–22] Although approaches like these have achieved much success in the improvement of membrane properties, they present drawbacks. For example, surface coatings may show low adhesive stability with the substrate and surface grafting processes may be complicated.

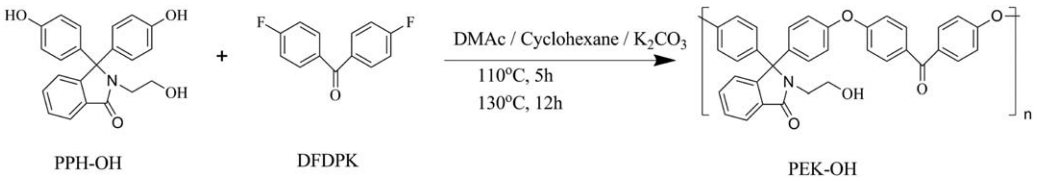


**Scheme 1.** Synthetic procedure of the polymer (PEK-OH). [Color figure can be viewed in the online issue, which is available at wileyonlinelibrary.com.]

Chemical modifications of the parent polymer, such as amination,[23,24] sulfonation,[25,26] carboxylation,[27,28] and chloromethylation,[29,30] have been used to impart hydrophilicity to the hydrophobic polymer. In contrast with post-modification of materials, polymerization of modified monomers and copolymerization with hydrophilic polymers represent strategies to control the molecular structure and avoid above problems because of single-step fabrication process.[31–33]

Phenolphthalein is a cardo bisphenol that contains a lactone group in its structure. This lactone group provides a reactive site with which to prepare various functional cardo bisphenols. Phenolphthalein-based cardo polymers are synthesized by polycondensation of bisphenol compounds and aromatic difluoro, dichloro, or dinitro compounds. We previously reported the synthesis of a series of phenolphthalein-based cardo poly (arylene ether sulfone) s containing different functionality, including phenyl, amino, and amide groups.[34–36] We also found that neutral zwitterionic poly (arylene ether sulfone)s with carboxybetaine groups or sulfobetaine groups had improved permeation and antifouling abilities.[37]

In this study, we devised a simple and efficient route to synthesize poly(arylene ether ketone) bearing hydrophilic hydroxyl groups (PEK-OH). PEK-OH was synthesized from 2-(2-hydroxyethyl)-3, 3-bis (4-hydroxyphenyl)-isoindolin-1-one (PPH-OH), and 4, 4′-difluorodiphenylketone (DFDPK) using annucleophilic substitution polycondensation reaction. PEK-OH ultrafiltration membranes were fabricated by phase inversion in a wet process. The water flux, BSA rejection, hydrophilicity, morphology, and chemical composition of the prepared membranes were studied. Furthermore, the antifouling capacity of the resultant membranes was measured both in the static and dynamic protein fouling experiments.

## EXPERIMENTAL

### Materials

Phenolphthalein was purchased from Beijing Chemical Reagent Company and used without purification. 2-Aminoethanol, N-methylpyrrolidone (NMP), dimethylsulfoxide (DMSO), dimethylformamide (DMF), and ethylene glycol monomethyl ether (EGME) was purchased from Beijing Chemical Works and used as received. 4,4′-Difluorodiphenylketone (DFDPK) was purchased from Changzhou Huashan Chemical Co. and dried at 60°C for 24 h via vacuum oven before used. N, N-dimethylacetamide (DMAc) was purchased from Xilong Chemical Co. and stirred over $CaH_2$ for 24 h, then distilled under reduced pressure, and stored over 4 Å molecular sieves. Anhydrous potassium carbonate ($K_2CO_3$) was dried at 100°C for 24 h before used. Poly(aryl ether ketone) cardo (PEK-C) with a weight-average molecular ($M_w$) of 124,000 g $mol^{-1}$ was supplied by our group. Commercial PES ultrafiltration membrane (UE50) was purchased from The Specialty Membrane Company. Bovine serum albumin (BSA, pI = 4.8, $M_w$ = 67 kDa) and lysozyme (LYZ, pI = 11.0–11.2, $M_w$ = 14.4 kDa) were purchased from Sino-American Biotechnology Co. Dextrans with different molecular weights (from 50,000 to 270,000 Da, Sigma) were used to characterize the molecular weight cut-off (MWCO) of ultrafiltration membranes.All other chemicals were reagent grade and used as received.

### Synthesis of Cardo Poly(arylene ether ketone) Bearing Hydroxyl Groups (PEK–OH)

The functional monomer PPH–OH was synthesized according to our earlier reported procedure.[38] As shown in Scheme 1, synthesis of cardo poly (arylene ether ketone) containing hydroxyol groups (PEK-OH) was accomplished by nucleophilic aromatic substitution polycondensation of PPH-OH and DFDPK. The typical procedure was as follows: to a flame dried 250 mL three-necked round-bottomed flask equipped with a Dean-Stark trap, mechanical stirrer and $N_2$ inlet, were added PPH-OH (10.8417 g, 0.03 mol), DFDPK (6.5460 g, 0.03 mol), anhydrous potassium carbonate (10.3590 g, 0.075 mol), 150 mL DMAc and 100 mL cyclohexane. The reaction mixture was heated with stirring at 110°C for 5 h. After cyclohexane and water had been removed by azeotropic distillation, the temperature was raised gradually and slowly to 130°C as well as kept at this temperature for 12 h to get a viscous solution. The mixture was cooled to room temperature and diluted with DMAc. The solution was centrifuged to remove inorganic salts. The filtrate was poured into water to give white flakes of the product, which were washed with hot water several times. The resulting product was dried under vacuum at 120°C for 24 h. Yield: 98%.

### Membranes Preparation

**Dense Membranes.** Dense membranes were prepared as follows: the polymer was dissolved in DMAc to form a 5.0 wt % solution. Then the polymer solution was filtered and degassed. After degassing, the viscous solution was cast onto a clean glass plate and the solvent was slowly evaporated over 12 h at 60°C. Residual solvent was thoroughly evaporated under vacuum for 24 h at 120°C. Then the membrane was immersed into deionized water and peeled off. Finally, the resulting dense membrane was dried for another 24 h at 120°C under vacuum before use.

**Asymmetric Flat Sheet Ultrafiltration Membranes.** The asymmetric flat sheet ultrafiltration membranes were prepared by the immersion coagulation phase inversion method. Membranes preparation steps were as follows: PEK-OH, DMAc, and ethylene glycol monomethyl ether (EGME) were dissolved at about 60°C for 10 h with vigorous stirring until the homogenous polymer solution was formed. After being filtered and degassed, the casting solution was cast onto the non-woven fabrics using the

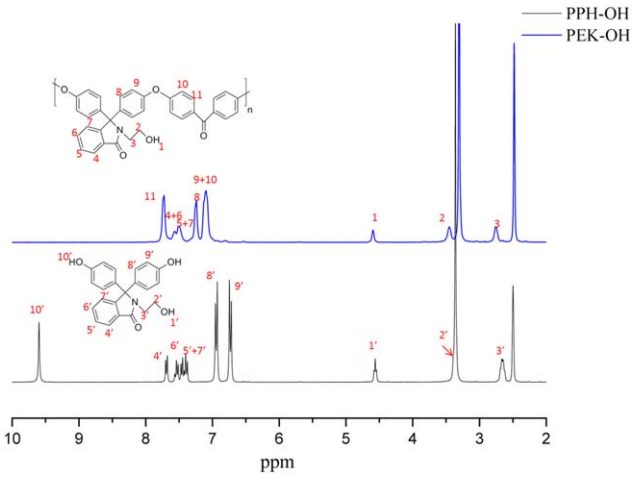


**Figure 1.** $^1$H NMR spectra of the monomer PPH and polymer PEK-OH in DMSO-$d_6$. [Color figure can be viewed in the online issue, which is available at wileyonlinelibrary.com.]

flat sheet membrane casting apparatus with a 190-μm blade and was precipitated by immersing into 20°C deionized water bath for 20 min; in order to replace the residual solvent completely by non-solvent water, the membrane was then immersed into 50°C water bath for 24 h.

The membrane performances and morphologies with different PEK-OH and EGME concentration were studied. The other specific preparation conditions were: (1) ambient humidity: 40%; (2) environmental temperature 20°C; (3) evaporation time: 3 s.

**Measurements**

The main functional groups of membrane were measured by Fourier transform infrared spectroscopy (FT-IR) (Bio-Rad digilab Division FST-80).Each spectrum was obtained in the region of 4000–500 $cm^{-1}$ and collected by cumulating 32 scans at a resolution of 4 $cm^{-1}$.

The proton nuclear magnetic resonance ($^1$H NMR) spectra were recorded in DMSO-$d_6$ on a Varian Unity spectrometer at 300 MHz at 30°C with tetramethylsilane as the internal.

Tensile measurements of the dense membranes were performed with a mechanical tester Instron-1211 instrument (Instron Co.) at a speed of 2 mm $min^{-1}$ at ambient humidity (approximately 30% relative humidity).

The surface and cross-section morphologies of flat sheet ultrafiltration membranes were observed using scanning electron microscopy (SEM, XL 30 ESEM FEG, FEI Company). The cross-section was obtained by fracturing the membranes in liquid nitrogen. All the samples were sputtered with gold prior to SEM measurement.

An atomic force microscopy (AFM, SPI3800N, Seiko instrumental) was used to analyze the surface topography. The AFM images were acquired in the tapping mode with silicone tip cantilevers. The root mean square (RMS) was used to evaluate the surface roughness of porous membranes based on 5.0 μm×5.0 μm scan area, and the images captured were compacted in 3D model and collected.

The static contact angles were recorded by the sessile drop method, using a Drop Shape Analysis DSA10 (KrüssGmbh, Germany) at ambient temperature. Water droplets (5 μL) were dropped carefully on to the surface of membranes with a micro-syringe. When the drop age was 10 s, the photo was taken and the contact angle was determined using imaging software. The resulting values were averages from measurements on at least 10 different positions for each sample.

X-ray photoelectron spectroscopy (XPS, ESCALAB 280 system) was used to analyze the surface compositions of membranes. Al/Ka ($h\nu$ = 1486.6 eV) was used as the X-ray source and dwell time and scanning was 100 ms and four times, respectively. The full range data was collected by survey scan (0–1000 eV, step size: 1). Narrow scan (step size:0.1) was conducted in the range of each atoms including carbon (C, 279.5–294.5 eV), oxygen (O, 527.9–542.9 eV) and nitrogen (N, 392.2–412.2 eV).

Molecular weight measurements were performed via gel permeation chromatography/light scattering(GPC/LS) at 30°C using an HPLC 515 pump equipped with Wyatt Optilab DSP and Wyatt DAWN EOS light scattering detectors. The separations

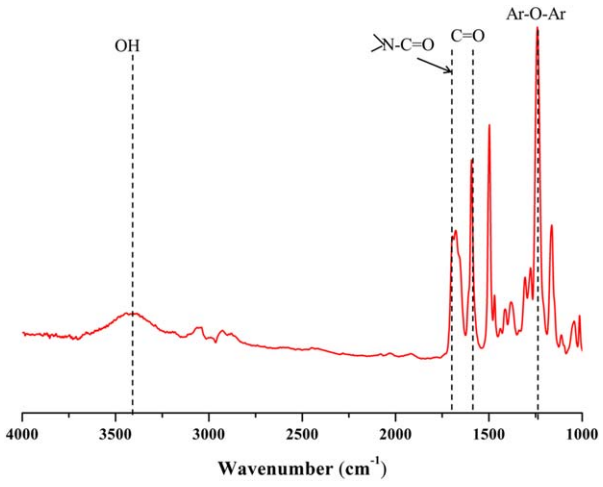


**Figure 2.** FT-IR spectrum of PEK-OH. [Color figure can be viewed in the online issue, which is available at wileyonlinelibrary.com.]

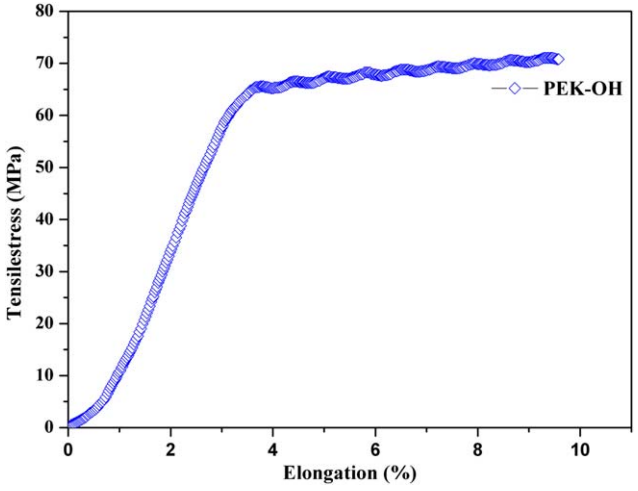


**Figure 3.** Mechanical properties of PEK-OH. [Color figure can be viewed in the online issue, which is available at wileyonlinelibrary.com.]

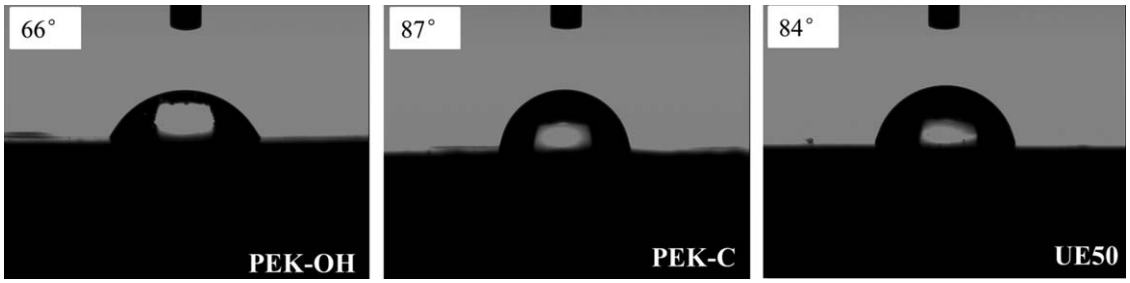


**Figure 4.** Contact angles images of PEK-OH, PEK-C and UE50 asymmetric membranes [Color figure can be viewed in the online issue, which is available at wileyonlinelibrary.com.]

were achieved in HMW 6E columns with 0.1 M LiBr in NMP as eluent at a flow rate of 1.0 mL·min$^{-1}$. $M_w$ and $M_n$ were calibrated with a polystyrene standard.

NDJ-1 type rotary viscometer (Yueping Scientific Instrument Co. Shanghai, China) was used to measure the viscosity of solutions at 25°C, with different PEK-OH and additive concentrations.

Density of polymer was measured by a density analysis instrument (Mettler Toledo, Switzerland). First, the temperature of surroundings was calculated by thermometer. Then, the weight of polymer in the air and in assistant liquid was measured, respectively. Finally, density of polymer was calculated by the instrument.

The membrane molecular weight cut off (MWCO)was carried out by filtration of different molecular weight dextrans solutions(from 50,000 to 270,000 Da) at same concentration. The concentrations of dextrans in feed and permeation were measured through a total organic carbon analyzer(TOC-VCPH SHIMADZU).All the measurements were based on three samples and adopt it average values.

The streaming potential measurement was done using an electrokinetic analyzer (SurPASS, Anton Paar GmbH, Austria). A pair of the prepared membranes having an area of 25–55mm$^2$ were placed in the measuring cell. The membranes were separated by a spacer that forms a streaming channel. The streaming potential was detected by the Ag/Ag Cl electrodes. A background electrolyte of 10 mM KCl solution was used and the pH was adjusted with 0.1M HCl and 0.1MNaOH. The zeta potential was obtained from the streaming potential using eq. (1).

$$\xi = \frac{\Delta E}{\Delta P}\frac{\eta\kappa}{\varepsilon\varepsilon_0} \tag{1}$$

where $\Delta E$ is the streaming potential, $\Delta P$ is the pressure drop across the streaming channel, $\varepsilon_0$ is the vacuum permittivity, $\varepsilon$ is the dielectric constant of the solution, $\eta$ is the solution viscosity, and $\kappa$ is the electrical conductivity of the bulk solution.

Membrane porosity and mean pore size were measured according to its dry weight. The wet membranes were vacuum dried at 60°C for 24 h and measured the dry weight. The porosity of membranes was calculated using the eq. (2).[39]

$$\varepsilon = \frac{V_m - V_p}{V_m} \times 100 \tag{2}$$

where $\varepsilon$ is the porosity of membrane, $V_m$ is the bulk volume of the membrane and $V_p$ represents the polymer volume. $V_m$ is obtained by multiplying the membrane area by its thickness. The volume occupied by the polymer ($V_p$) can be calculated by $W_m/\rho_p$, where $W_m$ is the weight of the membrane and $\rho_p$ is the density of polymer PEK-OH, PEK-C and has values of 1.248g·cm$^{-3}$and 1.231g·cm$^{-3}$, respectively.

The mean pore size ($r_m$) (nm) was calculated by Gueroult-Elford-Ferry equation [eq. (3)] on the basis of pure water flux and porosity data:[40,41]

$$r_m = \sqrt{\frac{(2.9 - 1.75\varepsilon)8\eta\delta_0 Q}{\varepsilon A \Delta P}} \tag{3}$$

where $\eta$ is the pure water viscosity ($8.9 \times 10^{-4}$ Pa s), $Q$ is the volume of the permeation of pure water per unit time (m$^3$·s$^{-1}$), $A$ (m$^2$ is the effective area of membrane, $\delta_0$ (m) is the thickness of membrane and $\Delta P$ is the trans-membrane pressure (100 kPa).

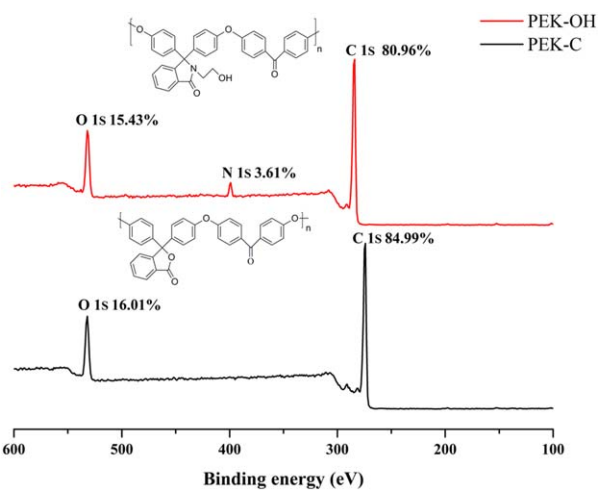


**Figure 5.** XPS spectra and composition elements content of PEK-OH and PEK-C membrane surface. [Color figure can be viewed in the online issue, which is available at wileyonlinelibrary.com.]

### Protein Static Adsorption

The amount of protein adsorbed to thePEK-OH, PEK-C, and UE50 asymmetric membranes were determined understatic exposure experiments. Bovine serum albumin (BSA, pI = 4.8, $M_w$ = 67 kDa) and lysozyme (LYZ, pI = 11.0–11.2, $M_w$ = 14.4 kDa) were chosen as model proteins for static adsorption. In a typical protein adsorption measurement, the membrane with 64 cm$^2$ of surface area was covered with 10 mL of 1 mg·mL$^{-1}$ protein solution (pH = 7.4, in 10 mmol phosphate-buffer). The protein solution

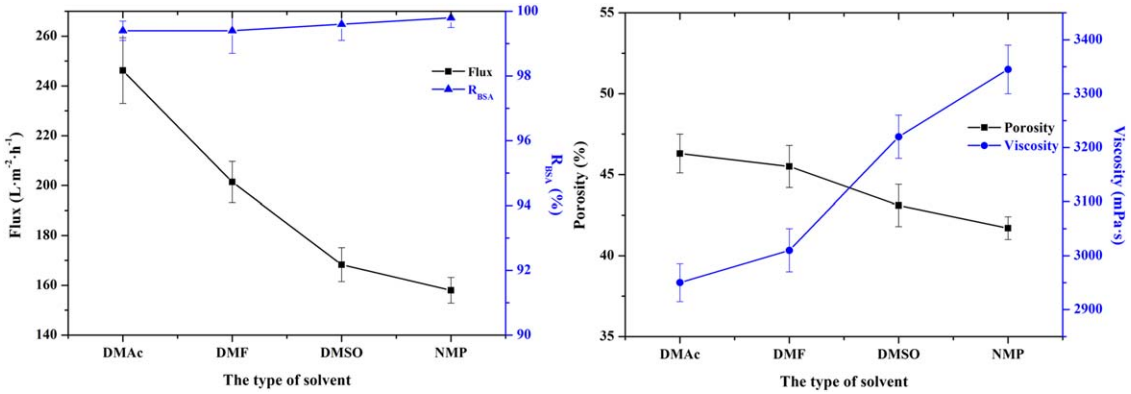


**Figure 6.** Influence of solvent on the resultant membrane properties. [Color figure can be viewed in the online issue, which is available at wileyonlinelibrary.com.]

was maintained at 25°C for 24 h with interval waving to reach an adsorption–desorption equilibrium. The amount of adsorbed protein was determined by UV spectroscopy at 278 nm from the concentration difference of before and after adsorption. The final results were averaged from three measurements for each kind of polymer membrane.

### Membrane Performance

Flat sheet ultrafiltration membranes were tested using a cross-flow filtration cell apparatus at 25°C, and the effective area of the membranes was 23.7 cm$^2$. First, the membrane was pre-compacted at 0.2MPa for 1 h. The pre-compaction process was conducted to achieve membrane compaction before the main filtration. Then the pressure decreased to 0.1MPa and all the ultrafiltration experiments were carried out at this pressure. Protein solution of 1000 ppm BSA used as standard solution for the rejection studies. The flux ($F$) could be calculated using the eq. (4).

$$F=\frac{V}{At} \tag{4}$$

where $V$ is the permeate volume (in L); $A$ denotes the effective membrane area (in m$^2$; $t$ is the testing time (in h). Protein rejection ratio ($R$) is expressed as eq. (5).

$$R(\%)=\left(1-\frac{Cp}{Cf}\right)\times 100 \tag{5}$$

where $C_p$ and $C_f$ (mg·mL$^{-1}$) are the concentrations of the permeation and the feed, respectively. The protein concentration of the permeation and feed were determined using a UV spectrophotometer at 278 nm.

### Fouling Evaluation of Membranes

1.0 mg·mL$^{-1}$ of BSA and LYZ solution were used as feed solutions for the fouling studies. Each membrane was initially compacted for 1 h at 0.2 MPa. Then the pressure was reduced to 0.1MPa and ensured the same pressure of PEK-OH, PEK-C, and UE50 ultrafiltration membranes. The initial pure water flux, Fw1 was calculated according to eq. (4). The cell was then emptied and refilled with BSA solution or LYZ solution. The steady state protein flux, $F_p$ after 3 h filtration was recorded. To evaluate the antifouling property of PEK-OH, PEK-C, and UE50 membranes, the flux decline rate was calculated by the following eq. (6).[42]

$$R_{fd}=\left(1-\frac{Fp}{F_{w1}}\right)\times 100\% \tag{6}$$

The degree of irreversible flux loss caused by irreversible fouling ($R_{ir}$) and reversible flux loss caused by reversible fouling ratio ($R_r$) is calculated using the following eqs. (7) and (8), respectively.[42]

$$R_{ir}=\left(\frac{F_{w1}-F_{w2}}{F_{w1}}\right)\times 100\% \tag{7}$$

$$R_r=\left(\frac{F_{w2}-F_p}{F_{w1}}\right)\times 100\% \tag{8}$$

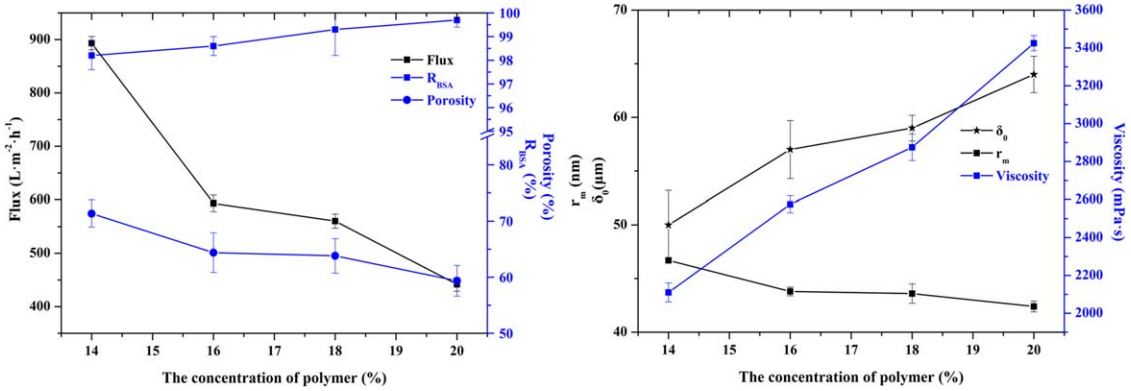


**Figure 7.** Influence of polymer concentration on the resultant membrane properties. [Color figure can be viewed in the online issue, which is available at wileyonlinelibrary.com.]

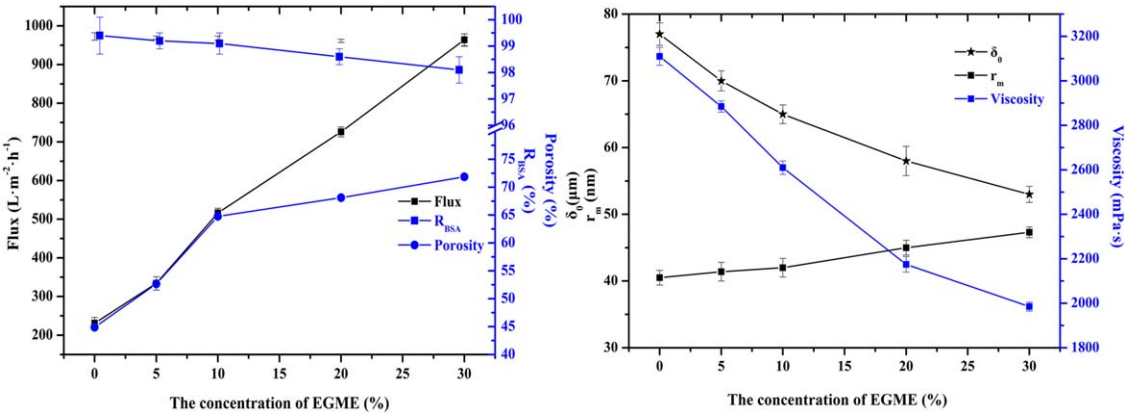


**Figure 8.** Influence of non-solvent additive EGME concentration on the resultant membrane properties. [Color figure can be viewed in the online issue, which is available at wileyonlinelibrary.com.]

The membranes after protein filtration were washed with deionized water for 1 h. After cleaning, the pure water flux of the membrane was measured (now denoted as $F_{w2}$). The operation was repeated for three cycles. The permeation through the membranes was measured every 10 min. To evaluate the anti-fouling property of the both membranes, the flux recovery ratio (FRR) is calculated using the following expression (9).[42]

$$\mathrm{FRR}=\left(\frac{F_{w2}}{F_{w1}}\right)\times 100\% \quad (9)$$

## RESULTS AND DISCUSSION

### Synthesis and Characterization of PEK-OH

Poly (arylene ether ketone) containing pendent hydroxyl groups (PEK-OH) was synthesized through the $S_NAr$ polycondensation of PPH-OH and DFDPK in the DMAc/$K_2CO_3$ system. And the synthetic route is outlined in Scheme 1. The synthesized polymer had good solubility and could be soluble in the common polar aprotic solvents such as DMF, DMAc, DMSO, and NMP. Gel permeation chromatography (GPC) demonstrated that a high-molecular-weight polymer was obtained, with an $M_n$ of $1.12\times10^5$ g·mol$^{-1}$, a $M_w$ of $1.32\times10^5$ g·mol$^{-1}$, and a polydispersity of 1.18.

The chemical structure of the monomer PPH-OH and the synthetic polymer PEK-OH were confirmed by $^1$H NMR spectroscopy with DMSO-$d_6$ as the solvent as depicted in Figure 1. There are remarkable changes in the $^1$H NMR spectra of the monomer PPH-OH and polymer PEK-OH. The spectrum of PPH-OH showed signal peak at 9.60 ppm (H10′), however, the peak was disappearing in the spectrum of PEK-OH. Furthermore, compared with the spectrum of PPH-OH, new peaks appear at 7.10 (H10) and 7.73 (H11) which correspond to the protons in the aromatic ring combined with carbonyl group. These indicated that the polymer PEK-OH was synthesized successfully by polycondensation reaction.

Typical FT-IR spectrum of the synthetic polymer PEK-OH was shown in Figure 2. For the polymer PEK-OH, characteristic adsorptions at 1240 cm$^{-1}$ (Ar-O-Ar), 1678 cm$^{-1}$ (conjugated carbonyl), 1695 cm$^{-1}$(N-phthalimide carbonyl), and 3404 cm$^{-1}$(-OH) were observed. In the curve, the peak of 1240 cm$^{-1}$(Ar-O-Ar) revealed the combination between PPH-OH and DFDPK.[37] It was suggested that the polymer PEK-OH was successfully synthesized.

### Mechanical Properties, Hydrophilicity, and Surface Composition of PEK-OH Membrane

As shown in Figure 3, the mechanical properties of dense polymer membranes were measured at room temperature and 30% relative humidity. Hydrophilic PEK-OH had a tensile stress of 73.0 MPa, a Young's modulus of 2.8 GPa, and an elongation at break of 9.5%. PEK-OH has good mechanical properties due to hydroxyl groups increasing the interaction between polymer molecules by hydrogen bonding. In laboratory level, good mechanical properties with tensile stress of 73–124 MPa, elongation at break of 9.7–12.8%, and tensile moduli of 2.2–2.8 GPa. Comparing with the benchmark, the tensile stress and elongation at break of synthesized PEK-OH located in the lowest value of the scope, however, the tensile moduli (2.8 GPa) of PEK-OH lay on the highest value.[43] Thus, the PEK-OH exhibited good mechanical properties.

The static water contact angles of PEK-OH, PEK-C, and UE50 asymmetric membranes are shown in Figure 4. The contact angle of PEK-OH membrane was 66.0 ± 2.4° lower than these

**Table I.** Summary of Performance of PEK-OH, PEK-C, and UE50 Ultrafiltration Membranes

| UF membrane | Flux (L·m$^{-2}$·h$^{-1}$) | $R_{BSA}$ (%) | $R_{LYZ}$ (%) | Porosity (%) | $r_m$ |
|---|---|---|---|---|---|
| PEK-OH | 516 ± 18 | 99.1 ± 1.4 | 85.3 ± 0.8 | 65.8 ± 1.3 | 42.0 ± 1.4 |
| PEK-C | 452 ± 12 | 94.7 ± 2.1 | 73.6 ± 1.1 | 63.7 ± 0.3 | 50.2 ± 0.7 |
| UE50 | 205 ± 7 | 99.7 ± 0.6 | 87.9 ± 1.3 | 47.4 ± 1.2 | 40.8 ± 1.9 |

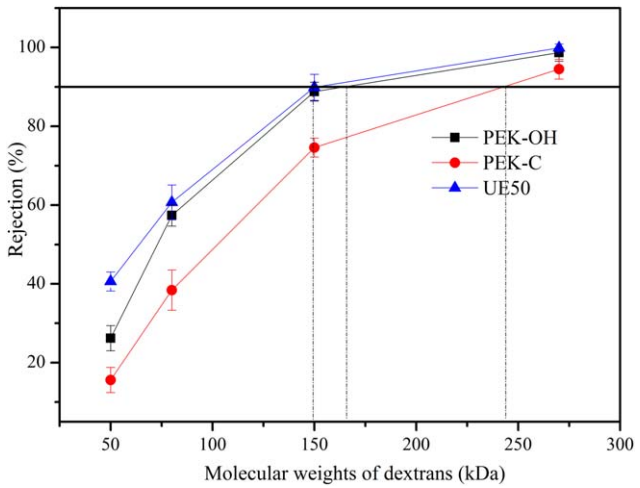


**Figure 9.** The MWCO curves of the PEK-OH, PEK-C, and UE50 by filtrating different molecular weight dextrans. [Color figure can be viewed in the online issue, which is available at wileyonlinelibrary.com.]

of the PEK-C membrane (87.0 ± 2.8°) and the UE50 membrane (84.0 ± 1.6°). This result indicated the hydrophilicity of PEK-OH was better than that of PEK-C and UE50.

X-ray photoelectron spectroscopy (XPS) spectra were used to analyze the surface composition of the PEK-OH membrane and the changes in chemical composition comparing with PEK-C membrane. Figure 5 showed the XPS spectra of PEK-OH membrane surface revealed the contents of carbon (C), nitrogen (N), and oxygen (O) elements were 80.96%, 3.61%, and 15.43%, respectively. Comparing with the XPS spectrum of PEK-C membrane surface, the sign of N element appeared on the XPS spectrum of the PEK-OH membrane, which clearly demonstrated that the hydrophilic side chain existed on the surface of the PEK-OH membrane.

### Preparation of an Asymmetric PEK-OH Membrane

**Selection of Solvent and Non-solvent Additive.** Predetermined amount of PEK-OH was dissolved in common polar aprotic solvents DMSO, NMP, DMF, and DMAc, respectively, to obtain a polymer content of 16 wt % without non-solvent additives. As seen from the Figure 6, the membrane prepared using DMAc as solvent exhibited the highest flux, without significantly sacrificing the rejection of BSA. The DMAc-based dope solution showed the lowest viscosity, which resulted in fast demixing. Therefore, it produced membranes with high porosity and flux. DMAc was selected as the membrane formation solvent in the next study.

In previous work, we found that the use of ethylene glycol monomethyl ether (EGME), which has good water miscibility and a high boiling point, as a non-solvent additive allowed us to achieve excellent membrane performance.[36] Therefore, EGME was selected as the non-solvent additive.

**Effect of Polymer and Non-Solvent Additive Concentration on Membrane Performance.** The membrane performance was investigated under the PEK-OH concentrations of 14, 16, 18 and 20 wt %, respectively. As shown in Figure 7, when the PEK-OH concentration increased from 14% to 20 wt %, the pure water flux decreased from 893 to 441 $L \cdot m^{-2} \cdot h^{-1}$. Meantime, the BSA rejection increased from 98.2% to 99.7%, correspondingly. Increasing the polymer content in the casting system led to a higher concentration of polymer at the nascent membrane interface with non-solvent, which yielded a denser surface layer, with lower flux, and higher rejection.[44] In Figure 7, the viscosity of the casting solution rose with the increasing of polymer concentration. The mass transfer rate of the non-solvent into the casting solution decreased due to the high viscosity, which resulted in lower porosity, increased membrane thickness ($\delta_0$) and decreased mean pore size ($r_m$).[45–47]

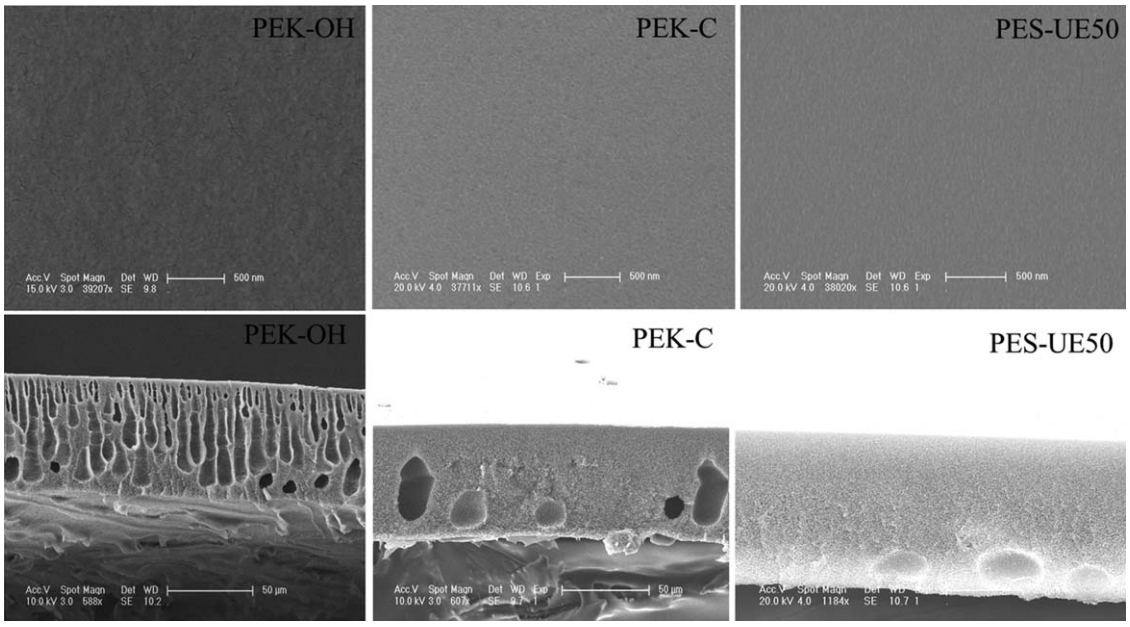


**Figure 10.** SEM surface (above) and cross-section (bottom) images showing morphologies of the PEK-OH, PEK-C, and UE50 ultrafiltration membrane.

**Table II.** Protein Static Adsorption on PEK-OH, PEK-C, and UE50 Ultrafiltration Membrane

| | BSA static adsoption | | | LYZ static adsorption | | |
|---|---|---|---|---|---|---|
| UF membrane | $A_b$ ($\mu$g cm$^{-2)}$ | $A_a$ ($\mu$g cm$^{-2}$) | $A_c$ ($\mu$g cm$^{-2}$) | $A_b$ ($\mu$g cm$^{-2}$) | $A_a$ ($\mu$g cm$^{-2}$) | $A_c$ ($\mu$g cm$^{-2}$) |
| PEK-OH | 102.31 | 99.19 | 3.12 | 97.23 | 93.19 | 4.04 |
| PEK-C | 102.31 | 13.6 | 88.71 | 97.23 | 8.06 | 89.17 |
| UE50 | 102.31 | 27.91 | 74.40 | 97.23 | 22.91 | 74.32 |

The polymer concentration was fixed at 18 wt % to get appropriate flux without obviously decreasing the rejection.

The effect of the non-solvent additive EGME on membrane performance was also investigated. Different amount of EGME with concentration of 0, 5, 10, 20, and 30 wt % was added to the dope solution, respectively. As shown in Figure 8, when the additive concentration increased from 0 to 30 wt %, the pure water flux increases from 231 to 964L·m$^{-2}$·h$^{-1}$. However, the rejection of BSA decreased from 99.4 to 98.1%. When instantaneous demixing occurs, the exchange rate of EGME and water is fast because EGME has good affinity with water. A higher concentration of EGME in the casting solution produced a membrane with higher porosity. On the other hand, the viscosity of the dope solution decreased from 3110 to 1985 mPa·s when the EGME content increased. The low molecular weight additive with intrinsic low viscosity would decrease the viscosity of casting solution. The trend was consistent with that demonstrated by several authors.[48,49] A decrease in the viscosity of the casting solution produced high porosity with a more polymer-lean phase at the point of precipitation, a decreased membrane thickness ($\delta_0$), and an increased mean pore size ($r_m$). An EGME concentration of 10 wt % was selected based on the performance of the different membranes.

### Membrane Anti-fouling Properties

**Static Antifouling Properties.** To investigate the anti-fouling properties of the fabricated membrane, static protein adsorption was conducted using BSA asa model protein. The PEK-OH membranes prepared using a dope solution composition of 18.0 wt % PEK-OH/10.0 wt % EGME/72.0 wt % DMAc and water as coagulant was used for study. One referenced PEK-C membrane was prepared using the same dope composition and membrane formation method.The performance of another compared UE50 membrane was also measured at the same condition. The comprehensive performances of the three kinds of membrane were listed in Table I. As seen from the Table I, the flux of PEK-OH ultratiltration is higher than PEK-C and PES membrane. There were two reasons about the phenomenon. One was that hydrophilic membrane enhanced water spreadability at same pressure. The other was that high porosity of membrane enhanced the permeability. The hydrophilicity and porosity of PEK-OH were higher than that of PEK-C and PES membrane. The rejection of BSA and LYZ for PEK-OH and PES membrane is similar and corresponds to the average pore size. Therefore, the choice of PES membrane as reference was appropriate. The MWCO curves of the three membranes are shown in Figure 9. It is depicted from the Figure 9 that the MWCO of PEK-OH, PEK-C and UE50 membrane is 165kDa, 245kDa, and 150kDa, respectively. This is in agreement with the BSA and LYZ rejection of the three membranes. Figure 10 shows the surface and cross-sectional morphologies of the PEK-OH, PEK-C, and UE50 flat sheet ultrafiltration membranes. The surface of PEK-OH, PEK-C, and UE50 membrane exhibited the similar morphology with typical closely packed nodules structure. And the cross-sections of the three membranes show distinct asymmetric structures: PEK-OH with a porous sublayer, which consists of polymer matrix and a finger-like macrovoid; however, hydrophobic PEK-C and PES membrane with a porous sponge-like sublayer. In general, if the hydrophilicity of polymer increases, usually a delayed demixing will happen and lead to the formation of sponge-like structure. So the improved hydrophilicity would not have been the only reason for the formation of macrovoids. The viscosity of PEK-OH polymer solution with 2610 mPaS is lower than that of PEK-C polymer solution with 2880 mPaS. Thus, in terms of kinetics the low viscosity solution leads to the quick exchange between water and solvent and generates finger-like structure.

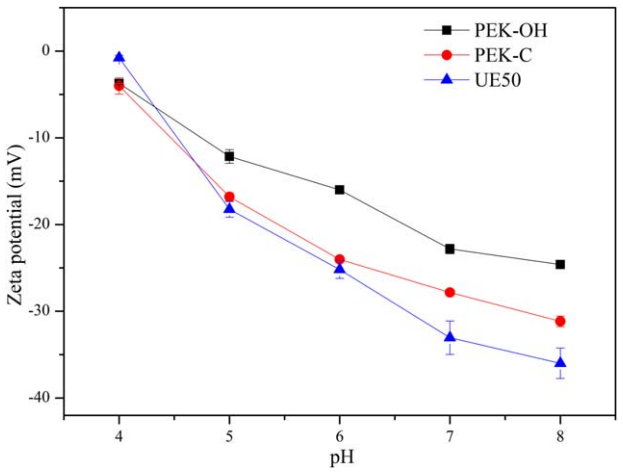


**Figure 11.** Zeta potentials of PEK-OH, PEK-C, and UE50 membranes at pH 4.0–8.0. [Color figure can be viewed in the online issue, which is available at wileyonlinelibrary.com.]

The static adsorption of BSA and lysozyme on PEK-OH, PEK-C, and UE50membrane with 64 cm$^2$ of surface area were investigated by exposing the studied membranes to a 1 mg·mL$^{-1}$ protein in phosphate-buffer solution at pH 7.4. The protein concentrations in the solution, before ($A_b$) and after ($A_a$) the static surface adsorption of the PEK-OH, PEK-C, and UE50 membrane are shown in Table II. According to the protein

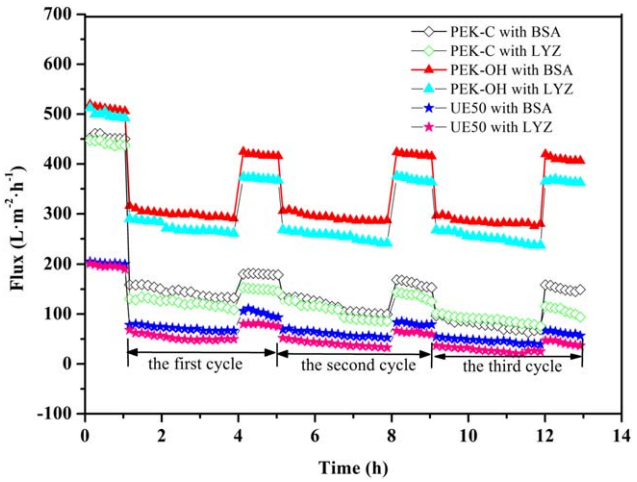


**Figure 12.** The time-dependent flux in three cycles of PEK-OH, PEK-C, and UE50 membranes in the 1.0 g $L^{-1}$ BSA or LYZ pH 7.4 phosphate-buffer solution filtration process. [Color figure can be viewed in the online issue, which is available at wileyonlinelibrary.com.]

concentration in the solution before and after static surface adsorption, the amount of protein adsorption ($A_c$) can be calculated. As seen from the Table II, the amount of BSA or LYZ protein adsorbed to the PEK-OH membrane was lower than the amount of protein adsorbed to the PEK-C and UE50 membranes. The amount of lysozyme protein adsorbed to the membrane surface was larger than that of BSA protein for the three membranes, indicating having an effect of different charge proteins adsorption on the membrane surface at pH 7.4 phosphate-buffer solution. In order to explain better about the adsorption of different charge proteins, the zeta potential of PEK-OH, PEK-C, and UE50 membranes varied with pH in Figure 11. All the membranes showed negative charge at between 4.0 and 8.0, although this membrane has no charge groups. Similar phenomena have been found, and it is ascribed to the specific adsorption of electrolyte anions onto the membrane surface.[50,51] Other explanation may be that the end group of polymer chain, for example phenolic hydroxyl group, showed negative charge. The amount of positive charge LYZ protein adsorbed on the negative charge membrane surface was larger than that of negative charge. Thus, the antifouling ability of the PEK-OH membrane is better than that of the PEK-C and UE50membrane.

**Dynamic Antifouling Properties.** To investigate the dynamic antifouling properties of the fabricated membranes, three-cycle filtration operations were conducted. The flux recovery curve was used to evaluate the hydraulic cleaning efficiency and fouling resistant abilities of the PEK-OH, PEK-C, and UE50 membranes. The initial flux values of the PEK-OH, PEK-C, and PES membranes were $516 \pm 18\ L{\cdot}m^{-2}{\cdot}h^{-1}$, $452 \pm 12\ L{\cdot}m^{-2}{\cdot}h^{-1}$, and $205.1 \pm 7\ L{\cdot}m^{-2}{\cdot}h^{-1}$ at 0.1 MPa. The flux and time-dependence curves for these membranes are shown in Figure 12. In the first hour of the pure water permeation process, the flux values were similar and decreased only because the membranes were compacted at pressure. The fluxes decreased sharply when the protein feed liquid took the place of pure water, because of the internal deposition of protein in the pores of the membranes and the formation of a filtration cake by the adsorption and deposition of protein on the membrane surface. Then, the ultrafiltration membrane was washed thoroughly and passed through deionized water for 2 h. It was worth noting that whether in BSA or LYZ solution filtration process, the hydrophilic PEK-OH had a smallest decrease than that of the hydrophobic PEK-C and UE50membrane. From the flux-time dependent curves, it could be seen that the PEK-OH membrane in BSA and LYZ filtration solution could achieve pure water flux recovery ratios 75% and 70% after three cycles of filtration, respectively. The flux recovery ratio of the new membrane described here higher than PSf-CS blend ultrafiltration (56%).[52] For the three kinds of membranes, a trend emerged that the flux in LYZ solution decreased much more than that in BSA solution. One reason was that when proteins entered into membrane pore in filtration process, the amount of low molecular weight LYZ was more than that of high molecular weight BSA. And proteins entering into pores were not washed away by hydraulic cleaning. Another was that the negative membrane adsorbed larger amount of positive LYZ protein.

To study their antifouling properties in more detail, the reversible and irreversible flux decline rates of the PEK-OH, PEK-C, and UE50 membranes were calculated. The results are presented in Table III. The flux decline ratio included two parts: an irreversible and a reversible fouling ratio. The irreversible fouling ($R_{ir}$) value of the PEK-C membrane was higher than that of the PEK-OH and UE50membrane and the flux decline occurred because of irreversible fouling. Irreversible fouling was caused by proteins entering into pores and not being washed away by hydraulic cleaning. Reversible fouling was caused by deposition and adsorption of proteins on the surface of the membrane. Reversible fouling can be easily removed, mostly by simply washing with water. The reversible fouling of the PEK-OH membrane was about two times that of the PEK-C and UE50 membranes because of the presence of a hydration layer on the PEK-OH membrane surface. Three-dimensional atomic force microscopy images of the initial PEK-OH, PEK-C, and UE50 membranes, as well as the fouled membranes are presented in

**Table III.** Summary of Antifouling Performance of PEK-OH, PEK-C, and UE50 Ultrafiltration Membranes

| | BSA filtration | | | | LYZ filtration | | | |
|---|---|---|---|---|---|---|---|---|
| Membrane | $R_{fd}$ (%) | FRR (%) | $R_r$ (%) | $R_{ir}$ (%) | $R_{fd}$ (%) | FRR (%) | $R_r$ (%) | $R_{ir}$ (%) |
| PEK-OH | 42.5 | 78.3 | 21.4 | 21.1 | 46.9 | 74.5 | 21.6 | 25.4 |
| PEK-C | 70.5 | 39.7 | 10.3 | 66.2 | 75.7 | 33.5 | 8.4 | 67.3 |
| UE50 | 66.8 | 46.7 | 13.3 | 53.5 | 73.8 | 38.2 | 13.1 | 60.7 |

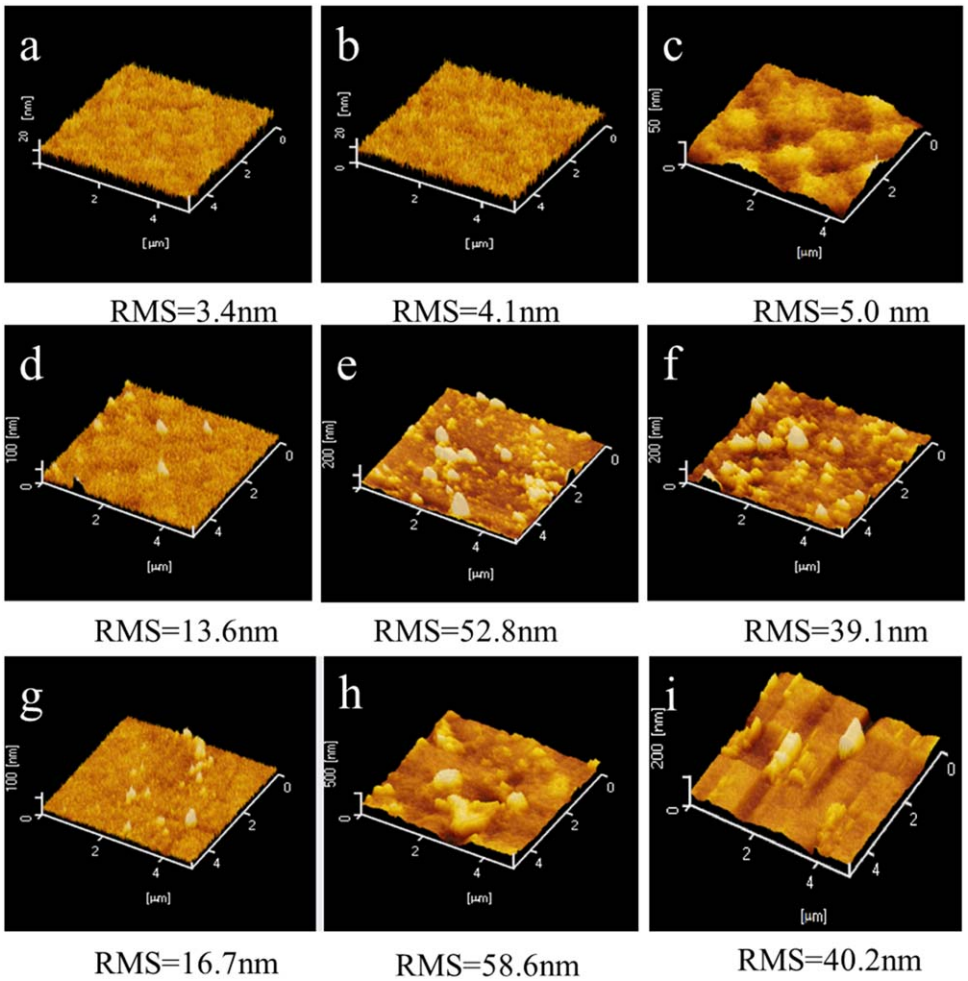


**Figure 13.** AFM three-dimension images of the PEK-OH (a,d,g), the PEK-C (b,e,h), and UE50 (c,f,i) membranes before (a,b,c) and after (d,e,f) BSA fouling, (g,h,i) LYZ fouling. [Color figure can be viewed in the online issue, which is available at wileyonlinelibrary.com.]

Figure 13. In these images, bright areas represent high points or nodules of the membrane surface and dark regions represent the valleys or membrane pores. Before filtering the BSA or LYZ solution, the roughness of the PEK-OH (a) membrane was similar to that of the PEK-C (b) and UE50 (c) membrane. After filtering the protein solution, all of these membranes were fouled and the roughness of the membranes became large. However, the roughness of LYZ-fouling surface was larger than that of BSA-fouling surface for all the membranes. The positive charge LYZ adsorbed easily on the negative charge membrane surface because of the electrostatic attraction. It was obvious that the roughness of the PEK-OH (d, g) membrane was lower than that of the PEK-C (e, h) and UE50 (f, i) membranes. It identifies that the hydrophilic surface of membrane plays a significant role in improving the membrane antifouling capacity. The surface of PEK-OH membrane can form a hydration layer which holds large amount of free water on the PEK-OH surface. Therefore, the fouling caused by protein molecules deposition into the pores and surface of membranes is decreased due to its hydration layer existing on the surface.[53] This result indicated that the hydrophilic PEK-OH membrane exhibited good antifouling property.

## CONCLUSIONS

An approach for a novel membrane formation polymer, poly (arylene ether ketone) with pendent hydroxyl groups (PEK-OH) was developed in this work. PEK-OH was synthesized from the new biphenol monomer PPH-OH and DFDPK using an $S_NAr$ polycondensation reaction. Ultrafiltration membrane that displayed high flux and good rejection was prepared using the optimized conditions. The amount of BSA adsorbed to the PEK-OH membrane was lower than the amount protein adsorbed to the referenced PEK-C and UE50 membranes. During a pressure-driven filtration process, the PEK-OH ultrafiltration membrane showed a 78.3% water flux recovery ratio, while only a 39.7% ratio and 46.5% were obtained with the PEK-C and UE50 ultrafiltration membrane in the first cycle of BSA filtration. However, the flux recovery ratio decreased separately to 74.5, 33.5, and 38.2% for PEK-OH, PEK-C, and UE50 membrane during LYZ filtration. After three cycles of BSA and LYZ filtration, the FRR of PEK-OH ultrafiltration membrane changed slightly to 75% and 73%, while that of PEK-C and UE50 ultrafiltration membranes remained declining gradually. This work demonstrated the successful usage of PEK-OH as antifouling membrane material.

## ACKNOWLEDGMENTS

This work was supported by the National Basic Research Program of China (grant 2015CB655302), the National Science Foundation of China (grants 51133008, 51203151, and 21074133), and the Development of Scientific and Technological Project of the Jilin Province (grant 20130204027GX).

## REFERENCES

1. Hendrix, K.; Koeckelberghs, G.; Vankelecom, I. F. J. *J. Membr. Sci.* **2014**, *452*, 241.
2. Han, R. L.; Zhang, S. H.; Yang, D. L.; Wang, Y. T; Jian, X. G. *J. Membr. Sci.* **2010**, *358*, 142.
3. Zarrin, H.; Wu, J.; Fowler, M.; Chen, Z. W. *J. Membr. Sci.* **2012**, *394-395*, 193.
4. Liu, W. Y.; Chen, T. L.; Xu, J. P. *J. Membr. Sci.* **1990**, *53*, 203.
5. Li, L. C.; Wang, B. G.; Tan, H. M; Chen, T. L; Xu, J. P. *J. Membr. Sci.* **2006**, *269*, 84.
6. Cui, Z. F.; Muralidhara, H. R. Membrane Technology; Elsiviler: London, **2010**; Chapter 1, p 12.
7. Suki, A. B.; Fane, A. G.; Fell, C. J. D. *J. Membr. Sci.* **1984**, *21*, 269.
8. Su, Y. L.; Li, C.; Zhao, W.; Shi, Q.; Wang, H. J.; Jiang, Z. Y.; Zhu, S. P. *J. Membr. Sci.* **2008**, *322*, 171.
9. Khan, F.; Ahmad, S. R. *Macromol. Biosci.* **2013**, *13*, 395.
10. Chen, X. R.; Su, Y.; Shen, F.; Wan, Y. H. *J. Membr. Sci.* **2011**, *384*, 44.
11. Meng, J. Q.; Li, J. H.; Zhang, Y. F.; Ma, S. N. *J. Membr. Sci.* **2014**, *455*, 405.
12. Revanur, R.; Closkey, B. M.; Breitenkamp, K.; Freeman, B. D.; Emrick, T. *Macromolecules* **2007**, *40*, 3624.
13. Kim, D. G.; Kang, H.; Han, S. S.; Lee, J. C. *J. Mater. Chem.* **2012**, *22*, 8654.
14. Ba, C. Y.; Economy, J. *J. Membr. Sci.* **2010**, *362*, 192.
15. Taniguchi, M.; Kilduff, J. E.; Belfort, G. *J. Membr. Sci.* **2003**, *222*, 59.
16. Sui, Y.; Gao, X. L.; Wang, Z. N.; Gao, C. J. *J. Membr. Sci.* **2012**, *394–395*, 107.
17. Wavhal, D. S.; Fisher, E. R. *Langmuir* **2003**, *19*, 6869.
18. Wei, Y. M.; Ma, J. J.; Wang, C. Z. *J. Membr. Sci.* **2013**, *427*, 197.
19. Yu, H. J.; Cao, Y. M.; Kang, G. D.; Liu, J. H; Li, M.; Yuan, Q. *J. Membr. Sci.* **2009**, *342*, 6.
20. Sui, Y.; Wang, Z. N.; Gao, X. L.; Gao, C. J. *J. Membr. Sci.* **2012**, *413–414*, 38.
21. Hu, M. X.; Yang, Q.; Xu, Z. K. *J. Membr. Sci.* **2006**, *285*, 196.
22. Yu, H. Y.; Liu, L. Q.; Tang, Z. Q.; Yan, M. G.; Wei, X. W. *J. Membr. Sci.* **2008**, *310*, 409.
23. Yang, Y. F.; Wan, L. S.; Xu, Z. K. *J. Membr. Sci.* **2009**, *337*, 70.
24. Jong, C. K.; Hwan, H. E.; Woo, Y. *Polymer* **2008**, *32*, 70.
25. Shen, L. Q.; Xu, Z. K.; Liu, Z. M.; Xu, Y. Y. *J. Membr. Sci.* **2003**, *218*, 279.
26. Li, Y.; Chung, T. S. *J. Membr. Sci.* **2008**, *309*, 45.
27. Wang, D. S.; Zou, W.; Sun, S. D.; Zhao, C. S. *J. Membr. Sci.* **2011**, *374*, 93.
28. Deng, B.; Yang, X. X.; Xie, L. D.; Li, J. Y.; Hou, Z. C.; Yao, S. D.; Liang, G. M.; Sheng, K. L.; Huang, Q. *J. Membr. Sci.* **2009**, *330*, 363.
29. Yan, X. M.; He, G. H.; Du, L. G.; Zhang, H. Y. *J. Membr. Sci.* **2011**, *15*, 204.
30. Li, L.; Wang, Y. X. *J. Membr. Sci.* **2005**, *262*, 1.
31. Liu, Y.; Yue, X. G.; Wang, G. B. *Appl. Surf. Sci.* **2010**, *256*, 7071.
32. Choa, Y. H.; Kima, H. W.; Parka, H. B. *J. Membr. Sci.* **2011**, *379*, 296.
33. Kumar, M.; Ulbricht, M. *RSC Adv.* **2013**, *3*, 12190.
34. Zheng, J. F.; He, Q. Y.; Gao, N.; Zhang, S. B. *J. Power Sources* **2014**, *261*, 38.
35. Chen, G.; Li, S. H.; Zhang, X. S.; Zhang, S. B. *J. Membr. Sci.* **2008**, *310*, 102.
36. Zhang, Q.; Li, S. H.; Zhang, S. B. *Chem. Commun.* **2010**, *46*, 7495.
37. Zhang, Q. F.; Dai, L.; Zhang, S. B.; Chen, X. S. *J. Membr. Sci.* **2010**, *349*, 217.
38. Zhang, Q.; Gong, F. X.; Zhang, S. B.; Li, S. H. *J. Membr. Sci.* **2011**, *367*, 166.
39. Tsai, H. A.; Ruaan, R. C; Wang, D. M.; Lai, J. Y. *J. Appl. Polym. Sci.* **2002**, *86*, 166.
40. Hamid, N. A. A.; Ismail, A. F.; Matsuura, T.; Zularisam, A. W.; Lau, W. J.; Yuliwati, E.; Abdullah, M. S. *Desalination* **2011**, *273*, 85.
41. Fan, X. C.; Su, Y. L.; Zhao, X. T.; Li, Y. F.; Zhang, R. N.; Zhao, J. J.; Jiang, Z. Y.; Zhu, J. A.; Ma, Y. Y.; Liu, Y. *J. Membr. Sci.* **2014**, *464*, 100.
42. Jayalakshmi, A.; Rajesh, S.; Mohan, D. *Applied Surface Sci.* **2012**, *258*, 9770.
43. Liu, J. T.; Chen, G. F.; Guo, J. C.; Mushtaq, N.; Fang, X. Z. *Polymer* **2015**, *05*, 058
44. Qin, P. Y.; Hong, X. J.; Shintani, T.; Chen, C. X. *Langmuir* **2013**, *29*, 4167.
45. Li, Z. S.; Jiang, C. Z. *J. Polym. Sci.: Part B: Polymer Physics* **2005**, *43*, 498.
46. Susanto, H.; Ulbricht, M. *J. Membr. Sci.* **2009**, *327*, 125.
47. Han, R. L.; Zhang, S. H.; Yang, D. L.; Jian, X. G. *J. Membr. Sci.* **2010**, *358*, 142.
48. Kim, I. C.; Lee, K. H. *J. Appl. Polym. Sci.* **2003**, *89*, 2562.
49. Zhang, Z. H.; An, Q. F.; Liu, T.; Zhou, Y.; Qian, J. W.; Gao, C. J. *Desalination* **2011**, *269*, 239.
50. Uchida, E.; Uyama, Y. K.; Ikada, Y. T. *Langmuir* **1994**, *10*, 1193.
51. Musale, D. A.; Kumar, A.; Pleizier, G. *J. Membr. Sci.* **1999**, *154*, 163.
52. Kumar, R.; Isloor, A. M.; Ismail, A. F.; Rashid, S. A.; Matsuura, T. *RSC Adv.* **2013**, *3*, 7855.
53. Yi, Z.; Zhu, L. P.; Xu, Y. Y.; Zhao, Y. F.; Ma, X. T.; Zhu, B. K. *J. Membr. Sci.* **2010**, *365*, 25.